Supporting Information

Controlled veiling of silver nanocubes with graphene oxide for improved SERS detection

Martina Banchelli,[a] Bruno Tiribilli,[b] Marella de Angelis,[a] Roberto Pini,[a] Gabriella Caminati,[c]* Paolo Matteini[a]*

[a] Institute of Applied Physics, National Research Council, via Madonna del Piano 10, I-50019 Sesto Fiorentino, Italy

[b] Institute for Complex Systems, National Research Council, via Madonna del Piano 10, I-50019 Sesto Fiorentino, Italy

[c] Department of Chemistry "Hugo Schiff" and CSGI, University of Florence, via della Lastruccia 3-13, I-50019 Sesto Fiorentino, Italy

*p.matteini@ifac.cnr.it, gabriella.caminati@unifi.it

Silver nanocubes (AgNCs) synthesis. AgNCs were prepared through a silver sulphide-induced polyol synthesis, by reducing silver nitrate dissolved in ethylene glycol in the presence of polyvinylpyrrolidone (PVP) with a trace amount of sodium sulphide at 150°C [1].

Immediately after the addition of silver nitrate, a fast reaction between sodium sulphide and silver nitrate occurs leading to the formation of cubic silver sulphide crystals, which act as catalyst for the subsequent formation of AgNCs. The colour of the reaction mixture undergoes rapid changes going from colourless to purple, yellow, orange, brown and metallic greenish brown in about 15 min. Small amounts of the reaction mixture were collected at different reaction times between 25 and 45 min and their absorption spectrum was registered (Figure S1). AgNCs typically show a main plasmonic peak at around 450 nm and two typical short-wavelength minor peaks (350 and 380 nm), according to previous reports [2]. A pronounced shoulder near 520 nm is observed when particles with different shape and size start to appear in the solution. The intensity of this shoulder had a minimum when the reaction time reached 40 min, which was thus chosen as optimal reaction time for the following experiments. The formation yield of the nanocubes as inferred from TEM analysis was >85% and the cube fraction had a rather narrow size distribution with an average value of 47±1 nm (Figures S2, S3).

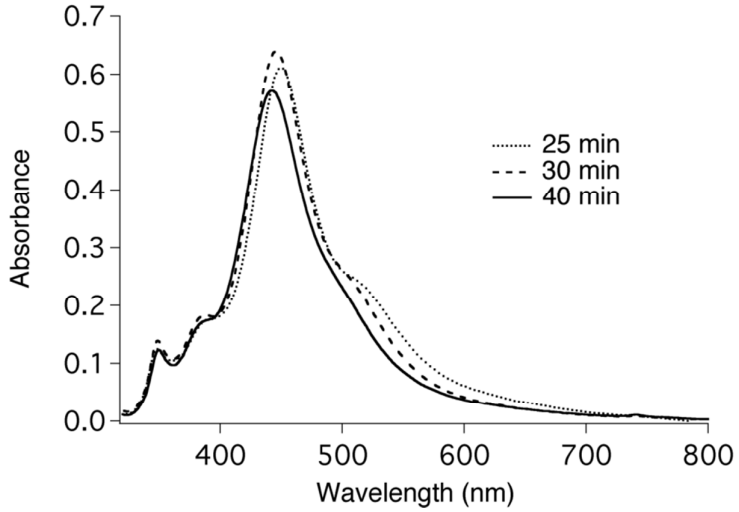

Figure S1. UV-vis spectra of AgNCs in ethanol obtained at different reaction times. UV-vis spectra of the nanocube suspension in ethanol and of monolayers deposited on quartz substrates were recorded using a Jasco V-6 UV-vis-NIR spectrophotometer with 1 nm slit and 200 nm min^{-1} scan rate.

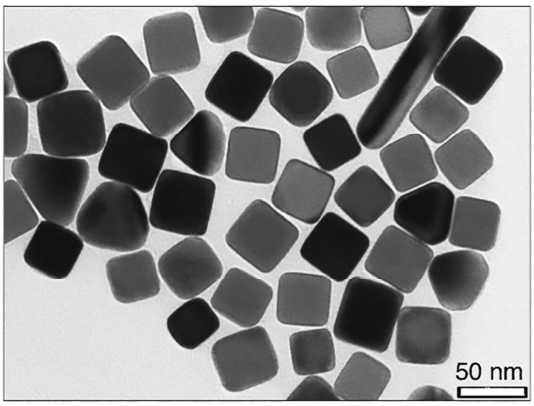

Figure S2. TEM image of AgNCs. TEM micrographs of the particles were acquired with a Philips CM-12 microscope running at 100 kV.

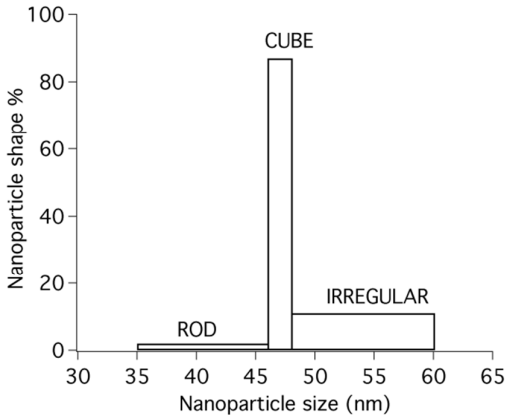

Figure S3. Distribution of the variability in shape and size of the synthesized nanoparticles. The lateral size is considered for rods.

Langmuir-Blodgett assembly. A chloroform dispersion of AgNCs was added dropwise to the water surface of a Langmuir trough and the packing density of the nanocubes was tuned by compression or expansion of the barriers of the trough while simultaneously recording surface pressure and the average surface area available to the nanocubes. The resulting pressure-area graph for the AgNCs monolayer shown in Figure S4 evidenced a monolayer behaviour that is usually observed for amphiphilic compounds, that is: a region of surface pressure invariance for large area values, where the nanocubes stay apart from each other, followed by an increase in surface pressure for decreasing areas [3,4]. As pressure rises, the particle density increases. Relaxation experiments at a constant surface pressure revealed a negligible area decrease in time (not shown) that excluded

loss of particles by diffusion toward the subphase, conferring reliability to the LB transfer process. Transfer of the AgNCs films at 5, 10, 15 and 20 mN m^{-1} (arrows, Figure S4) appeared always homogenous over the entire substrate surface. An optimal surface pressure of 15 mN m^{-1} was finally selected for transfer.

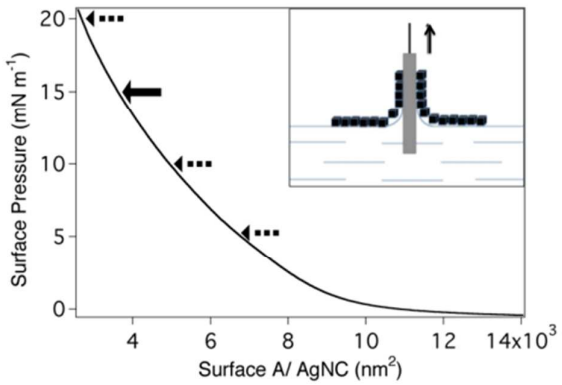

Figure S4. Changes to surface pressure as a function of average area available for each nanoparticle, leading to formation of monolayers. Arrows indicate the pressure values chosen for LB transfer. In the inset: schematic view of a LB transfer.

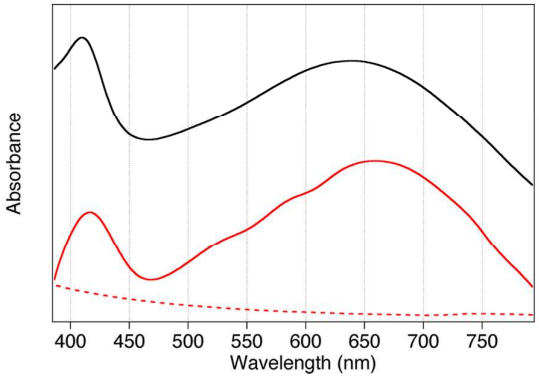

Figure S5. UV-vis absorbance spectra of AgNCs (black) and AgNCs@GO at 100 mg L^{-1} GO bulk concentration (red) assemblies. The spectrum of a GO dispersion (dashed red) is also shown for comparison. When compared to the AgNCs dispersion (Figure S1), shape and position of the blue band is noticeably blue-shifted (to ~410 nm) due to the lower dielectric environment of air with respect to solvent. The deposition of GO sheets onto the AgNCs film leads to a slight red-shift in the plasmon resonance at ~650 nm that may reflect a charge transfer between the metal nanoparticles and the GO layer.

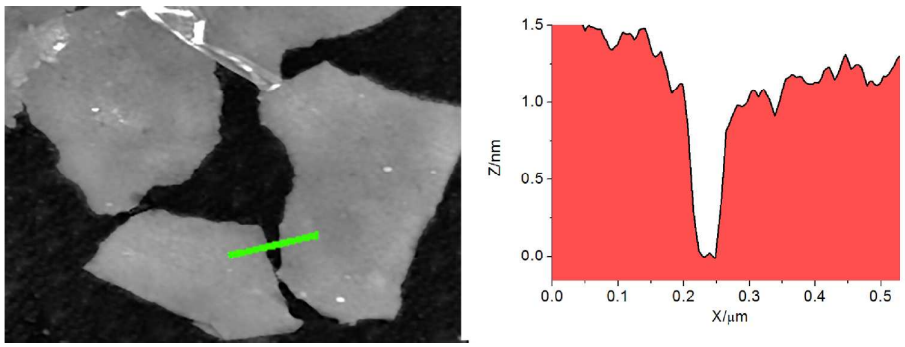

Figure S6. AFM topographic image of GO sheets.

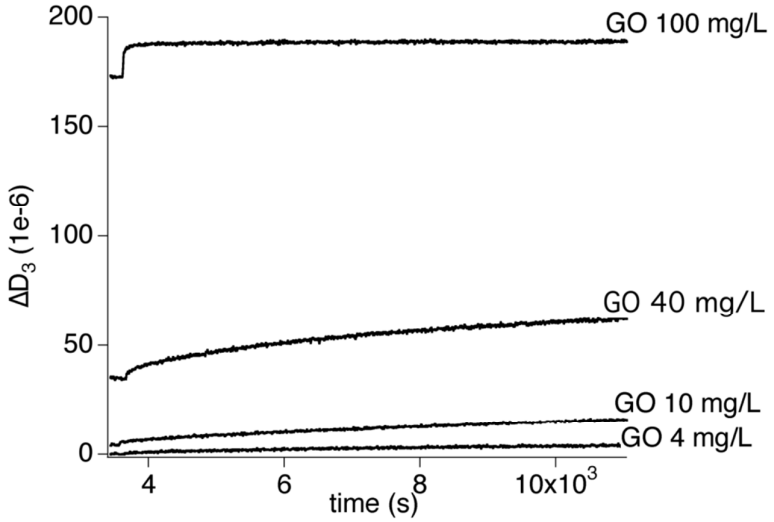

Figure S7. Dissipation shifts recorded during exposure of the AgNCs monolayers to aqueous dispersions of GO at different concentrations. Dissipation data are expressed as variation of the third harmonic of the dissipation factor D [5].

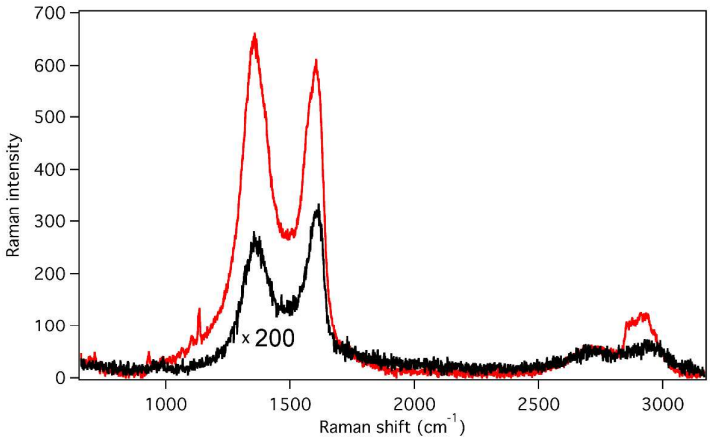

Figure S8. SERS profiles of GO adsorbed on a silicon wafer (black) and on a AgNCs assembly (red).

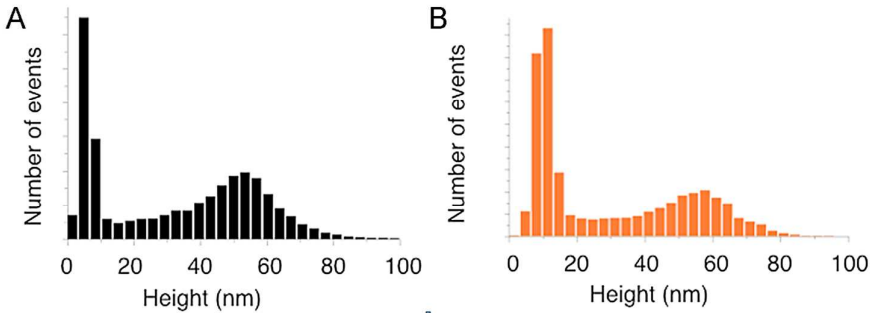

Figure S9. Height distribution of AFM profiles of bare AgNCs (A) and AgNCs covered by GO (B)

SERS Enhancement Factor. The SERS enhancement factor was calculated through the following equation :

$EF=N_{vol}I_{surf}/N_{surf}I_{vol}$,

where N_{vol} and N_{surf} are the number of molecules probed in the aqueous sample and on the SERS substrates, respectively; I_{vol} and I_{surf} are the corresponding normal Raman and SERS intensities of the Raman bands centred at 610 cm^{-1}. For the normal Raman signal, the probed volume was approximated as a cylinder with a diameter of 0.9 μm (diameter of focused laser) and a height of 6.3 μm (focus depth of laser). Considering the density of R6G powder (1.26 g cm^{-3}), the number of molecules being probed was calculated to be 5.8×10^9. When determining N_{surf} in the illuminated volume of our Raman setup, we assumed that R6G molecules were absorbed as a monolayer on the surface. The surface area of a single R6G molecule is ~2.0 nm^2, which was calculated considering a geometric area of 1.37 nm (length) × 1.43 nm (width). N_{surf} was then calculated to be 2.9×10^5.

The EF values for R6G 610 cm^{-1} band is larger than 10^5. This EF of our AgNCs@GO assemblies appeared comparable to larger to those previously reported for other Ag/GO nanocomposites [6].

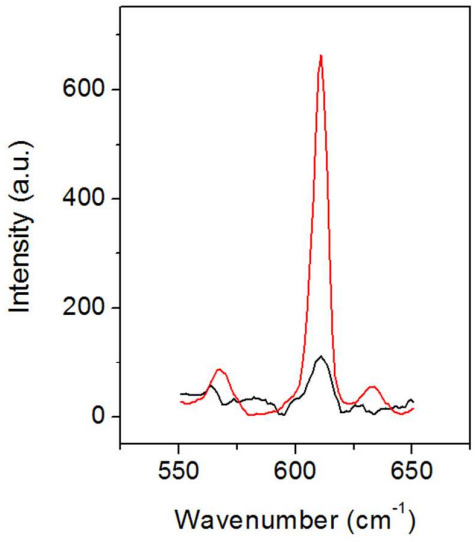

Figure S10. Comparison between the 610 cm^{-1} Raman (black) and SERS on AgNCs@GO substrates (red) bands of R6G

Finite Element Method modelling. Simulation of the electric field has been performed using a finite element method (FEM) under Comsol Multiphysics 4.4 software and operating in the scattering mode of the wave-optics-module to solve the Helmholtz equation. The local field enhancement factor was expressed in the form of normalized electric field intensity |E/E0|^2. Our geometry included a silver nanocube with 50 nm size surrounded by air and with a side covered by a GO layer. We considered two different thickness of the GO layer (1 nm and 7 nm), and a case without GO layer. In addition we calculated the electric field for 4 nanocubes as an exemplary geometry of clustered particles. In this case the cube-to-cube gap distance was set to 2 nm. The metal was described through its measured dielectric function [7], while the optical description of GO was based on [8]. The domains were delimited by perfectly matched layers (PML) in order to reach a close contact at the outer boundaries. The simulation have been done in 3D and the incident field was assumed to be an electromagnetic plane wave with linear polarization and 639 nm wavelength. Our experimental setup was with light at normal incidence onto the layer of nanocubes (light propagating along the z axis) and polarization along the y direction (see Figure 6).

References

1. A. R. Siekkinen, J. M. McLellan, J. Chen, Y. N. Xia, *Chem. Phys. Lett.* **2006**, *432*, 491-496

2. E. V. Panfilova, B. N. Khlebtsov, A. M. Burov, N. G. Khlebtsov, *Colloid. Journal.* **2012.**, *74*, 99-109

3. N. Ahamad, A. Ianoul, *J. Phys. Chem. C* **2011**, *115*, 3587-3594

4. M. A. Mahmoud, C. E. Tabor, M. A. El-Sayed, *J. Phys. Chem. C* **2009**, *113*, 5493-5501

5. F. Gambinossi, M. Banchelli, A. Durand, D. Berti, T. Brown, G. Caminati, P. Baglioni, *J. Phys. Chem. B* **2010**, *114*, 7338-7347.

6. W. Fan, H. Lee Y, S. Pedireddy, Q. Zhang, T. Liu, X. Y. Ling, *Nanoscale* **2014**, *6*, 4843-4851.

7. P.B. Johnson & R.W. Christy, *Phys. Rev. B* **1972**, 6, 4370-4379

8. BioNavis Ltd., *Application Note #116* **2015**